Seventh International Conference on CFD in the Minerals and Process Industries
CSIRO, Melbourne, Australia
9-11 December 2009

NUMERICAL ANALYSIS OF FLUID FLOW AND HEAT TRANSFER THROUGH A REACTIVE COAL STOKPILE

Arash EJLALI[1], S. M. AMINOSSADATI[2], and Azadeh EJLALI[3]

1,2 The University of Queensland, QLD 4072, Australia, E-Mail: a.ejlali@uq.edu.au

3 Department of Mathematics, University of Isfahan, Isfahan, Iran

ABSTRACT

The oxidation process occurring in stockpiles of reactive materials, such as coal, is a serious economic and safety problem. Due to the porosity of the stockpile, this flow behaviour is affected by the wind flow in the surrounding air. Comprehensive numerical solutions are derived from the governing Navier-Stokes and energy equations using the Brinkman-Forchheimer and the local thermal non-equilibrium (LTNE) porous model for the region occupied by coal. The effects of wind speed, porosity, permeability and variation of maximum temperature as the main criteria for spontaneous combustion have been investigated. To ensure the results are accurate, code validation and mesh independency have been applied. Two independent numerical solvers are used and cross-validated, these being a FORTRAN code and the commercially available software CFD-ACE. The results of this numerical modelling shows that the above mentioned parameters affect the air flow behaviour around the stockpile, maximum temperature inside the coal stockpile, and also the related heat removal at the interface of atmosphere and coal stockpile, which in turn alter the oxidation process of coal.

Keywords: Porous Media, Coal Stockpile, oxidation, Numerical

NOMENCLATURE

a_{sf} specific surface area of the packed bed, m^{-1}
c_p specific heat at constant pressure, J/(KgK)
d_p particle size, (m)
F inertial coefficient
h_{sf} fluid to solid heat transfer coefficient, W m^{-2} K^{-1}
h height of the computational domain, (m)
k thermal conductivity, (W/mK)
K permeability of the coal stockpile, (m^2)
L length of the computational domain, (m)
L dimensionless length of the computational domain
N normal direction to the coal stockpile side wall
Pe Peclet number, $(\rho_f C_p U_i t)/k_f$
Pr Prandtl number, $(\mu C_p/k_f)$
Q volumetric internal heat generation rate, (W/m^3)
Re Reynolds number, $(\rho_f U_i h)/\mu_f$
T stockpile bottom length, (m)
t Coal stockpile bottom length (m)
t* temperature, (K)
T dimensionless temperature, $(\mu C_p)(t*-t*_i)/(Qt^2)$
u streamwise velocity, (m/s)
U dimensionless streamwise velocity, u/U_i
U_i approaching (free stream) wind velocity, (m/s)
v velocity in transverse direction, (m/s)
V dimensionless velocity in transverse direction, v/U_i
x, y Cartesian coordinates, (m)
(X, Y) dimensionless Cartesian coordinates, (x/t, y/t)

GREEK SYMBOLS

ε porosity of the stockpile
μ fluid viscosity, (Pa.s)
ρ fluid density, (Kg/m^3)
γ shape parameter, $(t\sqrt{\varepsilon/K})$

SUBSCRIPTS

d dispersion
e effective
f fluid phase
i inlet condition
p porous
s solid phase
X,Y X,Y component of the vector

INTRODUCTION

Many mines and power generation companies around the world have to deal with spontaneous combustion of coal, which is a major problem creating difficulties in mining, storage and transportation. The term self-heating describes the phenomenon of a temperature rise in porous materials caused by the heat generated from chemical or physical processes taking place within the reactive porous material like coal stockpile. When the rate of heat generation within the stockpile becomes greater than the rate of heat dissipation to the environment, the temperature rise can become sufficiently high to cause the pile to ignite spontaneously and therefore self-heating acts as a precursor to spontaneous ignition. The amount of air entering the coal stockpile, as well as the coal temperature beyond which combustion is likely to happen, are two important parameters for the coal self heating study.

The self heating of coal stockpiles has been extensively studied in the past and some mathematical models have been developed to deal with this problem (JN Carras 1994; Koenning TH 1992; Salinger AG 1994).

A common solution is the protection of stockpiles with a barrier placed along the stockpile, although the effectiveness of this solution depends on the type of fluid regime, porosity and permeability. A main driving force for the process of self heating is the wind and coal oxidation which takes place as soon as coal comes into contact with oxygen. Wind creates airflow through the coal stockpile enhancing the oxidation process which in turn is affected by the diversity of compositions and properties of coal as well as its porous structure.

A review of the literature indicates a few numerical studies on the fluid flow and heat transfer by simulating coal as a porous material.(Ozdeniz AH 2008; Sensogut C 2002; Struminski A 2005; Zong-xiang LI 2008). In these studies, coal is assumed to have constant physical properties (porosity and permeability). This is not always a correct assumption. Struminski (Struminski A 2005) presented a method to determine the approximate temperature of an arising spontaneous fire centre and the time of coal self ignition. Ozdeniz and Sensogut (Ozdeniz AH 2008) experimentally investigated the effect of time, humidity, air temperature, air velocity and direction on the coal stockpile. A number of experimental and theoretical studies have shown that the variation of porosity near a solid boundary has a significant effect on the velocity fields in packed beds (Vafai k 1984, 1986; Vafai K 1985). This significantly affects the flow distribution, appearing as a sharp peak near the solid boundary and decreasing to nearly a constant value at the centre of the bed. This phenomenon is known as the channelling effect.

It is well documented in the literature that the study of thermal dispersion is essential for a number of applications in the transport processes through porous media. The effect of thermal dispersion on forced convection in fibrous media was reported by Hunt (Hunt ML 1988a). He investigated the non-Darcian flow and heat transfer through materials with different permeability, porosity and thermal conductivity. The results showed that the dispersion effect enhances heat transfer especially at high Reynolds numbers.

Some investigations have considered the effects of both thermal dispersion and variable porosity (Hong JT 1987; Hsu T 1990; Hunt ML 1988b). These studies aimed to correlate the experimental data to a formulation for the thermal dispersion conductivity or diffusivity, especially for relatively high speed fluid flow in porous media. Moghtaderi et al (Moghtaderi A et al. 2000)studied the effects of a dry wind-driven flow field on self heating characteristics and temperature variation within the constant property coal stockpile while neglecting the coal humidity. Krishnaswamy et al (Krishnaswamy S 1996) applied the forced convection model through open coal stockpile , and extended the problem to experimental and theoretical modelling by using fixed bed flow reactor. They used a two-dimensional model for spontaneous combustion of an open coal stockpile while the influence of moisture was neglected. Their calculation showed that the side slope, wind velocity and bed porosity significantly influence the prospects of long-term safe storage of coal in a stockpile. In this study, a coal stockpile has been numerically modelled as a porous media in order to examine the effects of wind speed, porosity, permeability and coal stockpile side angle on the maximum temperature of coal stockpile.

A FORTRAN code has been developed to solve the a system of governing equations including mass continuity, momentum, thermal energy equation (LTNE) including internal heat generation (Alazmi. B 2000).

MATHEMATICAL MODELLING

A diagram of the model geometry is shown in Figure 1. The coal stockpile has been modelled as a triangular homogenous two-dimensional porous medium. It is assumed that the solid and the fluid phase are not in local thermal equilibrium. A criterion, given by Nield (Nield 1998), was used for the validity of this assumption for the steady forced convection . The wind flow is assumed to be steady state, incompressible, and unidirectional as it approaches the stockpile. With these assumptions the general model of mass, momentum, and heat transfer cover both porous and non-porous domains.

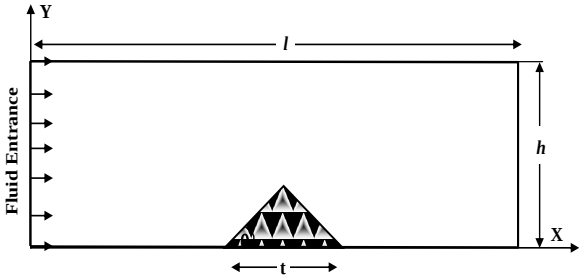

Fig. 1 Schematic diagram of the model geometry

The momentum and LTNE of energy equations throughout the porous medium can be presented by the following equations(Alazmi B and Vafai K 2000):

$$\frac{\partial V}{\partial t}+\frac{\rho}{\varepsilon}\langle(V.\nabla)V\rangle=-\frac{\mu}{K}\langle V\rangle-\frac{\rho F\varepsilon}{\sqrt{K}}[\langle V\rangle.\langle V\rangle]J+\frac{\mu}{\varepsilon}\nabla^2\langle V\rangle-\nabla\langle P\rangle \quad (1)$$

$$F=\frac{1.75}{\sqrt{150\,\varepsilon^3}} \quad (2)$$

$$K=\frac{\varepsilon^3 {d_p}^2}{150(1-\varepsilon)^2} \quad (3)$$

Fluid phase of energy equation.

$$(\rho c_p)_f\langle V\rangle.\nabla\langle T_f\rangle=\nabla.\{K_{feff}.\nabla\langle T_f\rangle\}+h_{sf}a_{sf}\langle T_s\rangle\langle T_s-\langle T_f\rangle\rangle \quad (4)$$

Solid phase of energy equation.

$$0=\nabla.\{K_{seff}.\nabla\langle T_s\rangle\}-h_{sf}a_{sf}\langle\langle T_s\rangle-\langle T_f\rangle\rangle+Q(1-\varepsilon \quad (5)$$

$$k_{f,eff}=\varepsilon k_f+k_d \quad (6)$$

$$k_{s,eff}=(1-\varepsilon)k_s \quad (7)$$

$$k_d=1.1\rho C_P U d_P \quad (8)$$

Although due to low speed fluid flow there is no need to consider dispersion effect.

The appropriate boundary conditions are

$$\text{X=0} \qquad U = 1, \quad V = 0, \quad \frac{\partial \psi}{\partial Y} = 1, \qquad \omega = \frac{\partial^2 \psi}{\partial X^2}, \quad T = 0 \tag{9}$$

$$\text{Y=0} \qquad U = 0, \; V = 0, \; \psi = 0, \qquad \omega = -\frac{\partial^2 \psi}{\partial Y^2}, \; \frac{\partial T}{\partial Y} = 0 \tag{10}$$

$$\text{Y=h/t} \qquad \frac{\partial U}{\partial Y} = 0, \; V = 0, \; \psi = Y, \qquad \omega = -\frac{\partial^2 \psi}{\partial Y^2}, \; \frac{\partial T}{\partial Y} = 0 \tag{11}$$

$$\text{X=L} \qquad \frac{\partial U}{\partial X} = 0, \qquad \frac{\partial V}{\partial X} = 0, \qquad \frac{\partial^2 \psi}{\partial X \, \partial Y} = 0, \quad \omega = -\frac{\partial^2 \psi}{\partial Y^2}, \; \frac{\partial T}{\partial X} = 0 \tag{12}$$

At the interface between porous layer and clear fluid the shear stress continuity equation has been adopted

$$\frac{\partial \overrightarrow{U_f}}{\partial N} = \frac{\partial \overrightarrow{U_p}}{\partial N} \tag{13}$$

NUMERICAL DETAILS

Numerical solutions to the governing equations for vorticity, stream-function, and dimensionless momentum equations are obtained by finite difference method (Tannehill et al. 1997), using the Gauss-Seidel technique with Successive Over Relaxation (SOR). To reduce the exit effect of computational domain, all lengths have been chosen long enough (l/t=20 and h/t=2). The governing equations are discretised by applying a second order accurate central difference schemes. The grid size in X and Y coordinates has been considered small enough to take all the velocity gradients. All runs were performed on a uniform 500 x 100 grid. Grid independence was verified by running two different grid sets 500 x 100, and 1000 x 200 to observe less than 2% difference between the results. The convergence criterion (maximum relative error in the values of the dependent variables between two successive iterations) in all runs was set at 10 E-6. The inertia coefficient is fixed at 0.56. The mesh cell diagonals have been rearranged in order to achieve a desirable triangular shape of stockpiles with different slopes and suitable compatible aspect ratios of mesh sizes in X and Y directions have been used. The above procedure was carried out to validate the FORTRAN code and repeated for the other solver being CFD-ACE where a triangular mesh system with a transition factor 1.05 and the minimum cell size of 10-5 was used. The maximum cell size was then changed from 0.1 to 0.01 to see that the results, based on these two different grids, are effectively the same. Figure 2 cross-validates the two numerical solvers for the highest Reynolds number, Re=100. As seen, the results for temperature distribution from the two solvers are in good agreement.

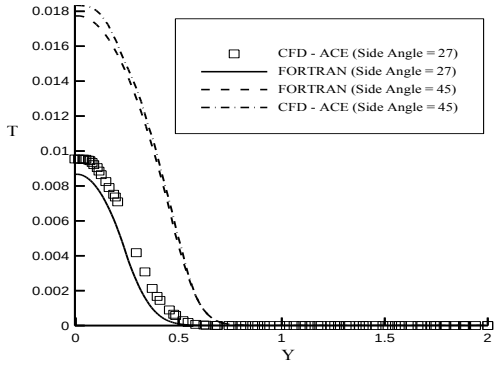

Fig. 2: Variation of T at X=5 for ε=0.4, K=10^{-7} m^2, and Re=100

RESULTS AND DISCUSSION

Streamlines and velocity vectors for five different Reynolds numbers and two coal stockpile side angles are shown in Figure 3. The streamlines deflect as the flow approaches the stockpile because of the higher flow resistance in this (porous) region compared to the non-porous area, and just a portion of air can penetrate the coal stockpile. As seen, for Re>10, and $\theta = 45^0$, a circulation zone can be observed just after the coal stockpile. This can be attributed to low permeability of the porous region that acts quite similar to a solid obstacle. By increasing the air velocity or air ratio (mass flow rate of air passing through the stockpile divided by the total approaching air mass flow rate), more heat is removed from the coal stockpile due to better heat removal at the pore level.

To study the temperature field inside the coal stockpile LTNE can be used by considering the internal heat generation. Figure 4 and 5 reveal the effect of air ratio on the maximum temperature of the coal stockpile for different porosities and two different coal stockpile side angles. Maximum temperature of the coal stockpile is a main criterion for the spontaneous combustion. The amount of air entering the coal stockpile as well as the coal temperature beyond which combustion is likely to happen are two important parameters to study for the coal stockpile self heating. By increasing the amount of air entering the stockpile, more heat is removed from the stockpile. Consequently, the maximum temperature inside the pile decreases. However, the oxidation process and the associated heating are enhanced. These figures show that the maximum temperature of coal stockpiles is inversely proportional with the air ratio, however a higher air ratio is not the best solution due to oxidation enhancement. The results also show that at a constant air ratio the maximum temperature of pile with the lowest possible porosity is much lower than the maximum temperature of coal with maximum porosity. It is the main reason for coal compaction and prevention of air flow through the stockpile in most coal industries.

Figure 6-a and 6-b show the effect of different Reynolds numbers (air ratio) on the maximum temperature of the stockpile and the air ratio. The former is a criterion for spontaneous combustion. That is, in practical applications, there is a certain coal temperature beyond

which combustion is likely to happen. The air ratio, on the other hand, as explained before, should be increased for better heat removal but the increase is favourable only if it does not boost the chemical reactions that in turn can increase the maximum temperature. So there is a trade off between introducing more air to the stockpile for better heat removal and the danger of oxidation. According to Fig. 6-a, the intersection between the two aforementioned opposing effects can be taken as the optimum design point between amount of air entering coal stockpile (air ratio) and coal stockpile maximum temperature. Obviously, the region just below this point can be considered as the safe zone when combustion is not likely to occur. Comparing the data of Fig. 6-a with those obtained for lower coal stockpile side angle, as depicted in Fig. 6-b, shows that this intersection (optimum) point moves down toward the abscissa. This, in turn, decreases the maximum temperature of coal stockpile.

CONCLUSION

A triangular coal stockpile with $\theta = 27^0$ and $\theta = 45^0$ have been modelled as a reactive porous media to study the fluid flow and maximum temperature variation., The effects of different porosities are studied on coal stockpile maximum temperature for different air ratios. Velocity vectors, streamlines for different Reynolds numbers are illustrated for better understanding of the problem. Numerical results showed that the maximum temperature of coal stockpile decreases as the air ratio increases. However, it must be taken into consideration that higher air ratio results in enhanced oxidation and associated heating process of coal. By decreasing the average porosity and increasing the air ratio, the lowest maximum temperature can be achieved when the coal oxidation process is taken into account. Air ratio enhancement improves the heat removal, but it also increases the coal oxidation process, so the intersection between air ratio and maximum temperature curves, when plotted versus Re, can be used to find out the safe (design) area in engineering applications.

REFERENCE:

ALAZMI B AND VAFAI K. 2000. "Analysis of Variants Within the Porous Media Transport Models " Journal of Heat Transfer 122:303-326.

ALAZMI. B, VAFAI. K. 2000. "Analysis of variants within the porous media transport models." Journal of Heat Transfer 122:303-326.

HONG JT, YAMADA Y, TIEN CL. 1987. "Effect of non-Darcian, non Uniform porosity on vertical plate natural convection in porous media." ASME Journal of Heat Transfer 109:356-362.

HSU T, CHENG P. 1990. "Thermal dispersion in porous medium " International Journal of Heat and Mass Transfer 33:1587-1597.

HUNT ML, TIEN CL. 1988a. "Effect of thermal dispersion in forced convection in fibrous media." International Journal of Heat and Mass Transfer 31:301-309.

HUNT ML, TIEN CL. 1988b. "Non-Darcian convection in cylindrical packed beds." ASME Journal of Heat Transfer 110:378-384.

JN CARRAS, ET AL. 1994. "Self heating of coal and related material: models, application and test methods." Prog Energy Combustion Sci 20:1-15.

KOENNING TH. 1992. "An overview of spontaneous combustion and recent heating in the western US,." Proc 9th Ann Int Pittsburgh Coal Conf:1081-1087.

KRISHNASWAMY S, ROBERT D, PRADEEP K. 1996. "Low Temperature Oxidation of Coal." Fuel 75(3):344-352.

MOGHTADERI A, DLUGOGORSKI Z AND KENNEDY M. 2000. "Effect of wind flow on self heating characteristics of coal stockpile." 78(Institute of chemical engineers, Trans IChemE).

NIELD, D. A. 1998. "Effects of local thermal nonequilibrium in steady convective processes in a saturated porous medium: Forced convection in a channel." Journal of porous media 1(2):181-186.

OZDENIZ AH, SENSOGUT C. 2008. "Modeling of coal stockpile using a finite elemnt method." Energy source, part A 30:723-733.

SALINGER AG, ARIS R, DERBY JJ. 1994. "Modeling of spontaneous ignition of coal stockpile." AIChE J 40(6):991-1004.

SENSOGUT C, KAUFMANN M, PETIT E. 2002. "An approach to the modelling of apontaneous combustion in the goaf." Journal of South Africa Institute of Mining and Metallurgy:311-319.

STRUMINSKI A, MADEJA-STRUMINSKA B. 2005. "Evaluation of arising spontaneous fire centre temperature and time of coal self ignition." Eighth International Mine Ventilation Congress:511-515.

TANNEHILL, JC, DA ANDERSON AND RH PLETCHER. 1997. Computational Fluid Mechanics and Heat Transfer 2nd Edition., 2nd Edition, US: Taylor and Francis.

VAFAI K. 1984. "Convective flow and heat transfer in variable porosity media." Journal of fluid mechanics 147:233-259.

VAFAI K. 1986. "Analysis of the channeling effect in variable porosity media " ASME Journal of Energy Resource Technology 108:131-139.

VAFAI K, ALKIRE R, TIEN CL. 1985. "An experimental investigation of heat transfer in variable porosity media." ASME Journal of Heat Transfer 107(642-647).

ZONG-XIANG LI. 2008. "CFD simulation of spontaneous coal combustion in irregular patterns of goaf with multiple points of leaking air." Journal of China Mining & Technology 18:504-508.

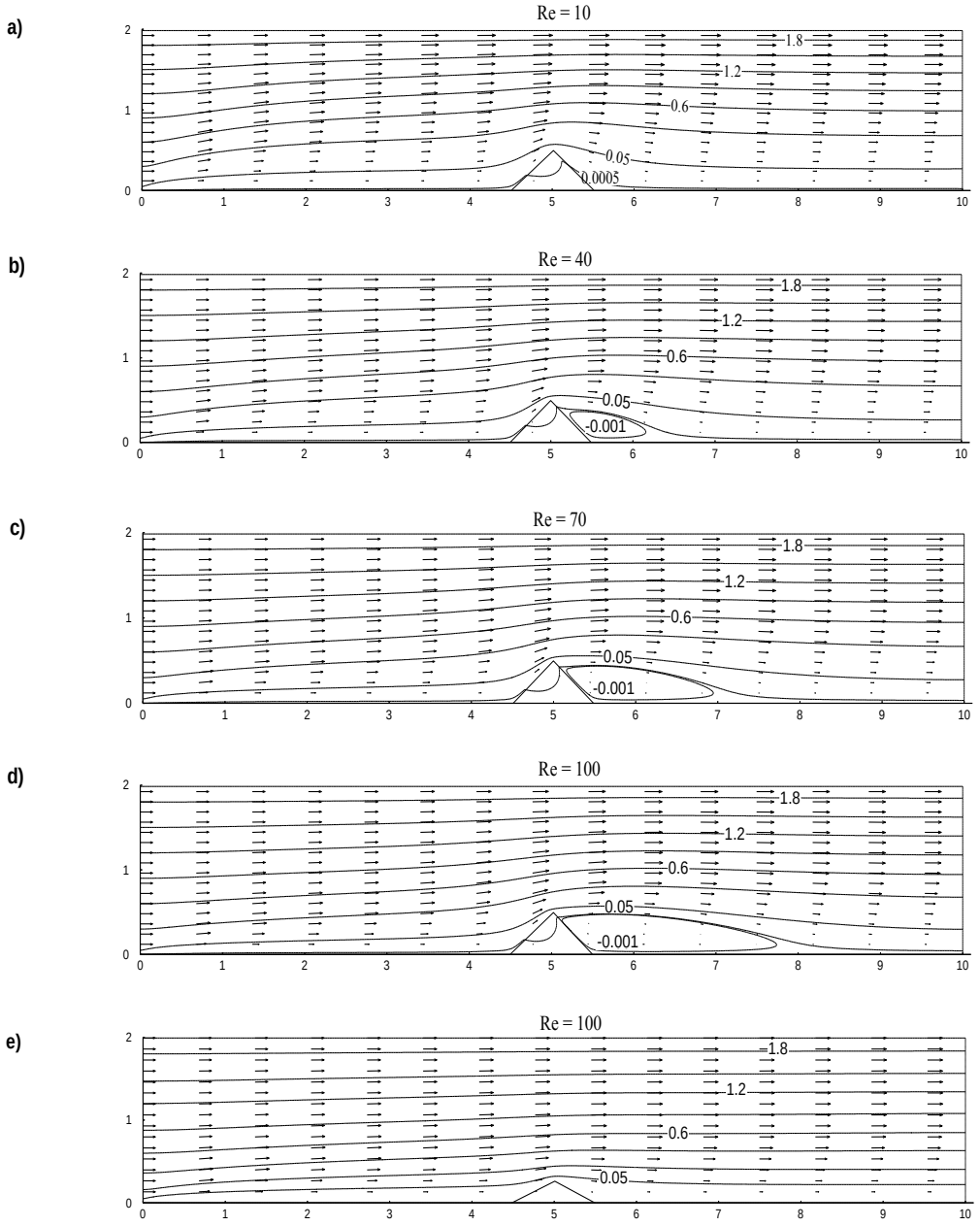

Fig. 3 Streamlines and velocity vectors for ε=0.4 and K=10-7 m2 a to d) $\theta = 45^{O}$ e) $\theta = 27^{O}$

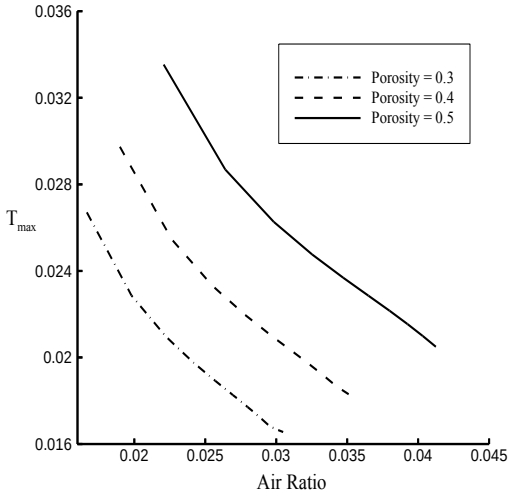

Fig. 4 Variation of maximum temperature versus air ratio using LTNE, $\theta = 45^{O}$, K=10-7 m2

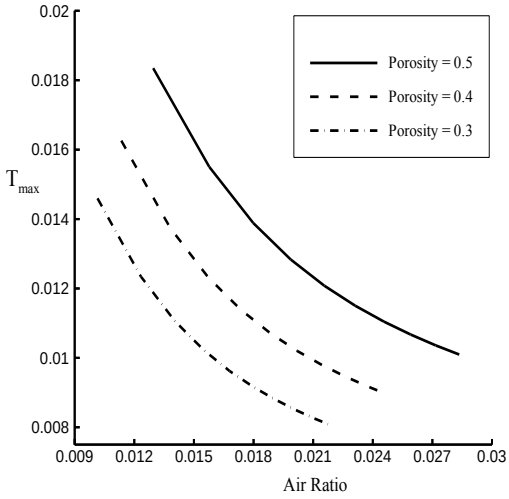

Fig. 5 Variation of maximum temperature versus air ratio using LTNE, $\theta = 27^{O}$, K=10-7 m2

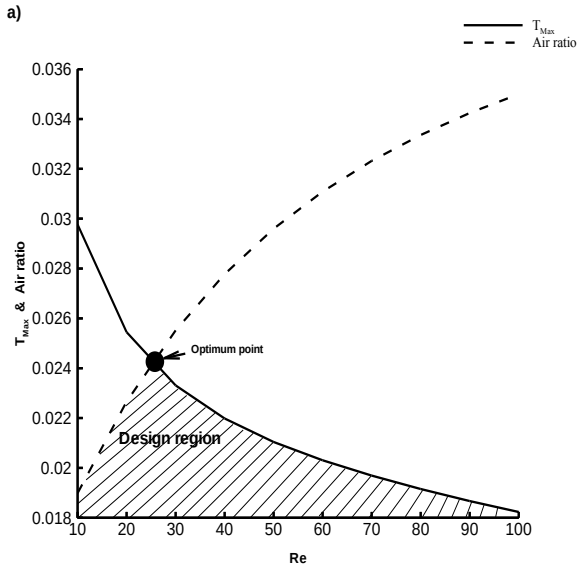

Fig. 6-a Optimum design point using LTNE $\theta = 45^{O}$, ε=0.4

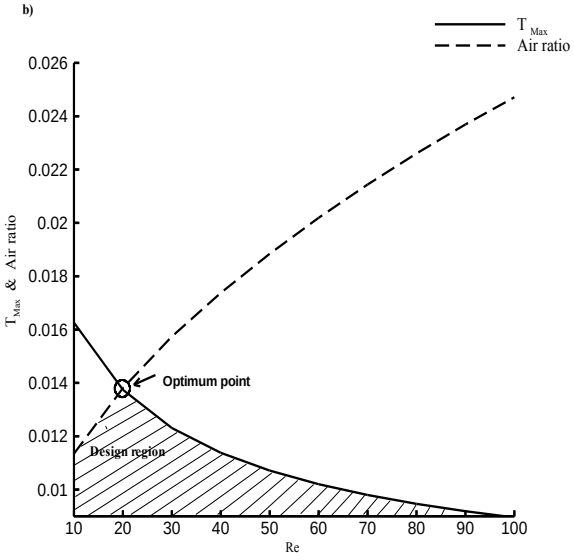

Fig. 6-b Optimum design point using LTNE $\theta = 27^{O}$, ε=0.4

